Potentiometric Determination of the Gibbs Energies of Formation of Lead Aluminates

W. W. Shim and K. T. Jacob

Email alerting service	Receive free email alerts when new articles cite this article - sign up in the box at the top right corner of the article or click here

4. J. Oroshnik and J. Kraitchman, *This Journal* **115,** 649 (1968).
5. H. Pogge, D. W. Boss, and E. Ebert, "Second International Conference on Chemical Vapor Deposition," J. M. Blocher and J. C. Withers, Editors, The Electrochemical Society Softbound Proceedings Series, Princeton, NJ (1972).
6. J. Dierres and A. Spiro, Abstract 62, p. 161 (1974).
7. J. Chruma and P. Hilton, U.S. Pat. 900,597 (1975).
8. J. Duchemin, Thesis, Université de Caen, France 1976.
9. T. Kamins, *This Journal,* **127,** 686 (1980).
10. A. Baudrant and M. Sacilotti, Note Interne Th/ EFCIS DRD 80-21, Grenoble, France, 1980.
11. T. Kamins, *This Journal,* **126,** 838 (1979).
12. F. Faggin and T. Klein, *Solid State Electron.,* **13,** 1125 (1970).
13. T. O'Connel, IEEE International Solid State Circuits Conference, Philadelphia, Paper WAM 1.2., February 1977.
14. A. and M. Meinel, *Physics Today,* **25,** 44 (February 1972).
15. T. Kamins, *IEEE Trans. Parts, Hybrids and Packing,* **php-10,** 221 (1974).
16. T. Kamins, M. M. Mandurah, and K. C. Saraswat, *This Journal,* **125,** 927 (1978).
17. W. Brown and T. Kamins, *Solid State Technol.,* **22,** 51 (1979).
18. J. Seto, *This Journal,* **122,** 701 (1975).
19. Y. Yasuda, M. Yamanaka, T. Moriya, and T. Yoshii, Paper 23 presented at the Electrochemical Society Meeting, Houston, TX, May 7-11, 1972.
20. M. Hammond, *Solid State Technol.,* **22** (12), 61 (1979).
21. K. Chiang, C. J. Dell'Oca, and F. N. Schwettman, *This Journal,* **126,** 2267 (1979).
22. H. Splittgerber *et al.,* "Semiconductor Silicon 1977," H. R. Hull and E. Sirtl, Editors, p. 253, The Electrochemical Society Softbound Proceedings Series, Princeton, NJ (1977).
23. S. Horinchi, *Solid State Electron.,* **18,** 1111 (1975).
24. J. Duchemin, M. M. Bonnet, and M. F. Koelsch, *This Journal,* **125,** 637 (1978).
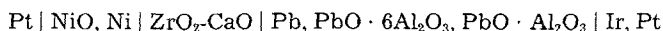25. M. Cowher and T. Sedgwick, *ibid.,* **119,** 1565 (1972).

Potentiometric Determination of the Gibbs Energies of Formation of Lead Aluminates

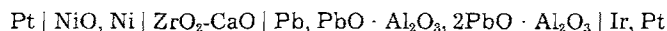## W. W. Shim* and K. T. Jacob**

Department of Metallurgy and Materials Science, University of Toronto, Toronto, Ontario, Canada M5S 1A4

ABSTRACT

The Gibbs energies of formation of three compounds in the PbO-Al_2O_3 system—$2PbO \cdot Al_2O_3$, $PbO \cdot Al_2O_3$, and $PbO \cdot 6Al_2O_3$—have been determined from potentiometric measurements on reversible solid-state galvanic cells

$$Pt, Ir \mid Pb, \alpha\text{-}Al_2O_3, PbO \cdot 6Al_2O_3 \mid ZrO_2\text{-}CaO \mid NiO, Ni \mid Pt$$

$$Pt \mid NiO, Ni \mid ZrO_2\text{-}CaO \mid Pb, PbO \cdot 6Al_2O_3, PbO \cdot Al_2O_3 \mid Ir, Pt$$

and

$$Pt \mid NiO, Ni \mid ZrO_2\text{-}CaO \mid Pb, PbO \cdot Al_2O_3, 2PbO \cdot Al_2O_3 \mid Ir, Pt$$

in the temperature range 850-1375 K. The results are discussed in the light of reported phase diagrams for the PbO-Al_2O_3 system. The partial pressures of different lead oxide species, Pb_nO_n, $n = 1$-6, in the gas phase in equilibrium with the aluminates are calculated by combining the results of this study with the mass-spectrometric data of Drowart *et al.* (1) for polymerization equilibria in the gas phase. The concentration of oxygen in lead in equilibrium with the aluminates are also derived from the results and the literature data on the Gibbs energy of solution of oxygen in liquid lead.
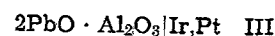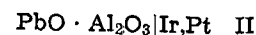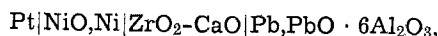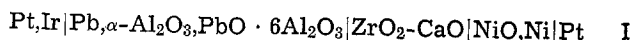
Alumina is commonly used as a container or structural material in furnaces for the manufacture of lead zirconate titanate (PZT) ceramics. During the sintering operation, lead-containing species are present in the gas phase and they can react with alumina with possible formation of $2PbO \cdot Al_2O_3$, $PbO \cdot Al_2O_3$, and/ or $PbO \cdot 6Al_2O_3$. The partial pressure of PbO determines the type of compound most likely to form.

Close control of the sintering operation is very critical for optimizing the properties of PZT ceramics. The electrical properties of the product are highly dependent on stoichiometry. The stoichiometry in turn depends on the partial pressures of volatile components and on the duration of heat-treatment. The reaction of structural or container materials with the gas species results in their depletion and lower pressures. Thermodynamic and kinetic data on the formation of lead aluminates would be useful for a more detailed analysis and control of high temperature processing of PZT ceramics.

In the earliest study of the PbO-Al_2O_3 system by Geller and Bunting (2) only one compound, $PbO \cdot$

Al_2O_3, was identified. Subsequently, Torkar *et al.* (3) identified two additional compounds, $2PbO \cdot Al_2O_3$ with monoclinic symmetry and $PbO \cdot 6Al_2O_3$, usually described as lead β-alumina due to its structural analogy to magnetoplumbite. More recent work by Kuxman and Fischer (4) has confirmed the existence of all three compounds in this system.

This paper reports measurements on the Gibbs energies of formation of lead aluminates using solid-state galvanic cells incorporating the calcia-stabilized zirconia electrolyte. The cells used can be represented as

$$Pt, Ir \mid Pb, \alpha\text{-}Al_2O_3, PbO \cdot 6Al_2O_3 \mid ZrO_2\text{-}CaO \mid NiO, Ni \mid Pt \quad \text{I}$$

$$Pt \mid NiO, Ni \mid ZrO_2\text{-}CaO \mid Pb, PbO \cdot 6Al_2O_3,$$

$$PbO \cdot Al_2O_3 \mid Ir, Pt \quad \text{II}$$

$$Pt \mid NiO, Ni \mid ZrO_2\text{-}CaO \mid Pb, PbO \cdot Al_2O_3,$$

$$2PbO \cdot Al_2O_3 \mid Ir, Pt \quad \text{III}$$

where the negative electrodes are on the left side. Similar solid-state cells have been used to measure the Gibbs energies of formation of lead zirconate (5) and titanate (6).

Experimental Methods

Materials.—The three lead aluminates were synthesized from their component oxides. Fine powders of orthorhombic yellow PbO (99.9% pure) and α-Al_2O_3 (99.9% pure) were dried under a pressure of 10^{-2} Pa at 450 K overnight. The oxides were mixed in molar ratios of 1:6, 1:1, and 2:1 using a mortar and pestle. The oxide mixtures were compacted into pellets at 30 MN m^{-2} to ensure intimate contact of reactant particles. The pellets of each composition were placed in closed platinum crucibles. These crucibles were then placed in larger ZrO_2-CaO crucibles provided with lids. The space between the two crucibles was packed with a mixture of PbO and Al_2O_3 of the same composition as the pellet. The double encapsulation was used to minimize the volatilization of PbO from the mixtures. The heating and cooling rate of the crucibles was set at 400 K hr^{-1}; at or below this rate cracking of ZrO_2-CaO crucibles due to thermal shock was not a problem. The highest temperatures that could be used for synthesis without significant loss of PbO from the samples or the formation of a liquid phase depended on their composition. The pellets containing PbO and Al_2O_3 in the molar ratio of 1:6 were heated up to 1400 K for 3 hr and then homogenized at 1100 K for 12 hr. Pellets containing an equimolar mixture of PbO and Al_2O_3 were heated to 1200 K for 3 hr and then homogenized at 1100 K for 12 hr. Samples containing PbO and Al_2O_3 in the ratio 2:1 were heated to a maximum temperature of 1100 K for 3 hr, followed by heat-treatment at 1000 K for 12 hr. The pellets were then reground, repelletized, and the heating cycle was repeated once on each sample. The identity of the final products was confirmed by x-ray diffraction analysis. Some samples were chemically analyzed. The results showed small loss of PbO during synthesis resulting in composition changes less than 0.6%.

Apparatus and procedure.—A schematic diagram of the cell assembly is shown in Fig. 1. Zirconia stabilized by the addition of 15 mol percent (m/o) CaO, obtained from the Zircoa Corporation, was used as the solid electrolyte in the form of one-end closed flat-bottomed tubes, 11 mm outer diameter. Metallic lead along with an equimolar mixture of two neighboring oxide phases in PbO-Al_2O_3 system was placed inside the zirconia tube. The two oxide phases establish a unique activity of PbO at this electrode. The electrical lead to this electrode was provided by an iridium wire, approximately 2 cm long, which did not react with the molten lead or lead aluminates. The iridium lead was spot-welded to a platinum wire, protected from lead vapors by shielding inside an alumina tube sealed by alumina cement. The Ir-Pt junction was maintained in the constant temperature zone of the furnace (± 3 K) and therefore did not contribute a thermoelectric emf.

The reference electrode was a mixture of Ni and NiO in the molar ratio of 2:1. This reference electrode, placed in an alumina crucible, was spring-loaded against a coil of Pt-wire and the outside of the zirconia electrolyte. An additional amount of Ni + NiO mixture was packed around the solid electrolyte tube after the alumina crucible containing the reference electrode was in place.

The cells were operated under dried Ar gas (99.999% pure) flowing at a rate of 2-10 ml sec^{-1} over each electrode. Residual oxygen in the inert gas stream was removed by a copper getter placed upstream from the cell inside the furnace tube at a position where the temperature was approximately 750 K.

To check for the correct functioning of the apparatus, the potential of the cell

$$Pt|NiO,Ni|ZrO_2\text{-}CaO|Pb,PbO|Ir,Pt \qquad IV$$
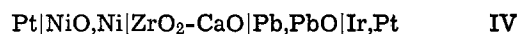
was measured as a function of temperature and compared with values reported in the literature. The potentials agreed with values reported by Jacob and Jeffes (6) within ± 2 mV. On prolonged exposure (>30 hr) to temperatures in excess of 1300 K, the emf began to drift gradually to lower values. Visual and x-ray examination of cell components after an exposure of approximately two days indicated a small amount of lead zirconate on the electrolyte tube near the melt/gas interface

$$(1 - x)PbO + ZrO_2 \rightarrow Pb_{1-x}ZrO_{3-x} \qquad [1]$$
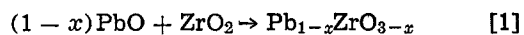
where the nonstoichiometric parameter x has a value of 0.0995 at 1373 K (8). At lower temperatures and for shorter exposures at high temperatures, there was no evidence of reaction between sintered tubes of ZrO_2-CaO and PbO.

Results

The open-circuit potentials of the cells were independent of the flow rate of Ar gas in the range 2-10 ml sec^{-1}. At higher flow rates, differential cooling of the electrodes causes a small flow rate dependence. The cells displayed constant potentials in 30-60 min after an increase in temperature. The cell response was much more sluggish when the temperature was decreased; 3-12 hr were required to attain steady potentials. The solubility of oxygen in liquid lead decreases significantly with temperature (9). Pure PbO is precipitated when the temperature of the cell is rapidly decreased. The precipitated PbO must completely react with oxides at the electrode before the cell can register the correct potential.

Coulometric titrations of oxygen through the zirconia electrolyte were performed to check the reversibility of the cells. A current of ~60 μA was passed through the cell for 2 min in either direction. Then the external voltage was removed and the cell was allowed to come to equilibrium under open-circuit conditions. The steady-state potentials after titration were found to be equal, within ± 2 mV, to that registered before the titrations. Generally, a potential remaining constant over 60 min is considered to be the steady-state value.

The highest temperatures of operation were 1375 for cell I, 1275 K, for cell II, and 1225 K for cell III. The potentials were not reproducible above these temperatures. The reversible potentials of these cells are plotted as a function of temperature in Fig. 2-4. Within experimental error, the emf's appear to be linear func-
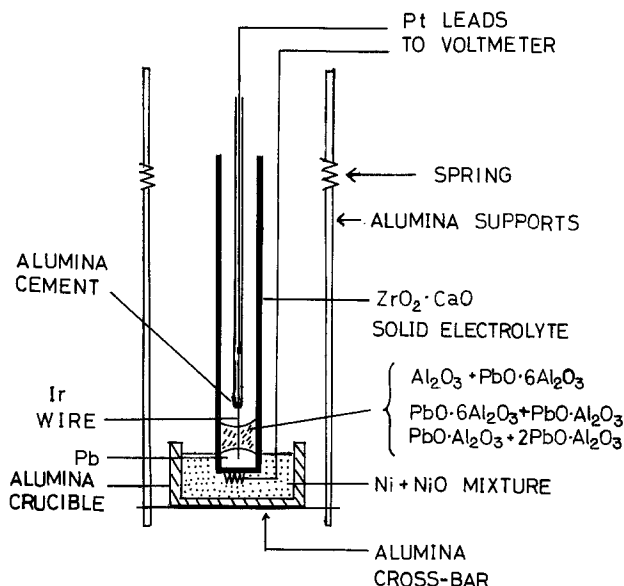

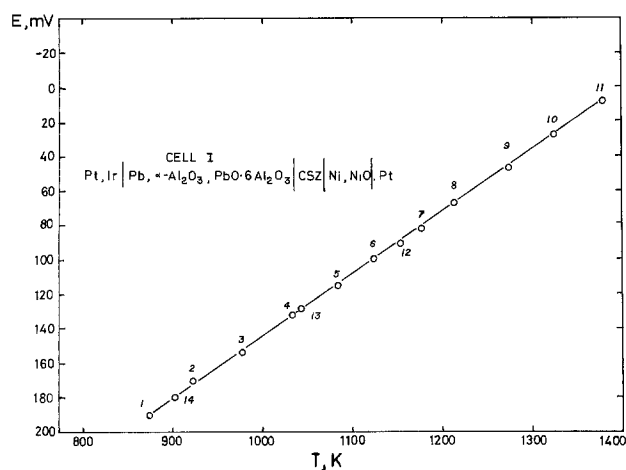Fig. 1. A schematic diagram of the apparatus used in this study

Pt LEADS
TO VOLTMETER

SPRING

ALUMINA SUPPORTS

ALUMINA CEMENT

ZrO_2·CaO
SOLID ELECTROLYTE

Ir WIRE

Al_2O_3 + PbO·6Al_2O_3
PbO·6Al_2O_3 + PbO·Al_2O_3
PbO·Al_2O_3 + 2PbO·Al_2O_3

Pb

ALUMINA CRUCIBLE

Ni + NiO MIXTURE

ALUMINA CROSS-BAR

Fig. 2. The temperature dependence of open-circuit potential of cell I. The experimental points are numbered to indicate the sequence of measurements.
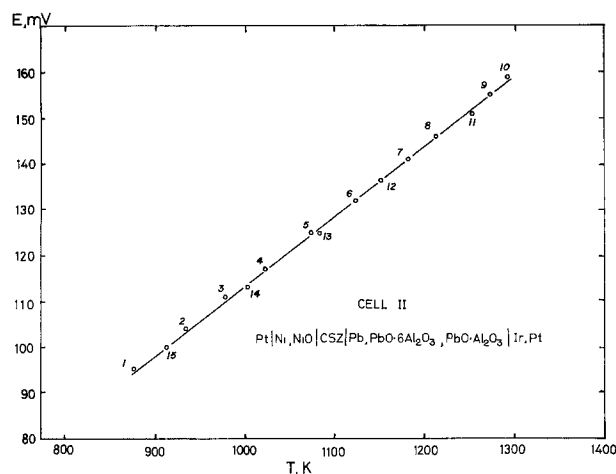

Fig. 3. The variation of the potential of cell II with temperature
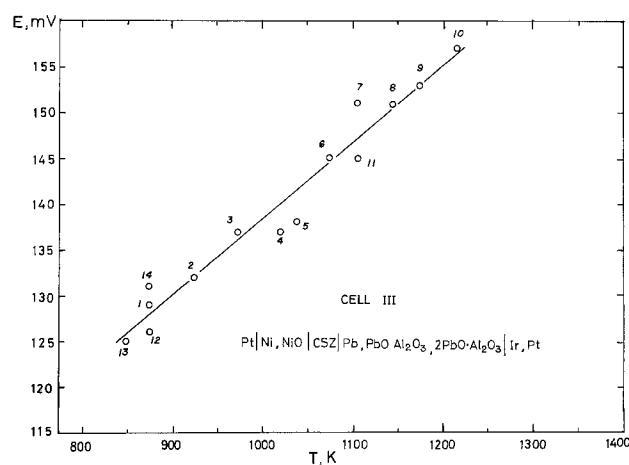

Fig. 4. The temperature dependence of the potential of cell III

tions of temperature. The least-mean-squares analysis gives the following equations

$$E_I, \text{mV} = 506.4 - 0.3618T \ (\pm 1), \ (875\text{-}1375 \ \text{K}) \quad [2]$$

$$E_{II}, \text{MV} = -38.14 + 0.1516T \ (\pm 1), \ (875\text{-}1275 \ \text{K}) \quad [3]$$

$$E_{III}, \text{mV} = 54.82 + 0.0836T \ (\pm 2.5), \ (850\text{-}1225 \ \text{K}) \quad [4]$$

$$E_{IV}, \text{mV} = 83.2 + 0.0725T \ (\pm 2), \ (750\text{-}1130 \ \text{K}) \quad [5]$$

The uncertainty limits correspond to twice the standard deviation. The oxide phases in equilibrium with lead at the electrodes of cells I to III were examined after each experiment by x-ray diffraction. The diffraction patterns for the aluminates were identical to those for stoichiometric samples prepared from component oxides. This suggests that the aluminates do not exhibit significant nonstoichiometry.

Discussion

Gibbs energies of formation of $2PbO \cdot Al_2O_3$, $PbO \cdot Al_2O_3$, *and* $PbO \cdot 6Al_2O_3$.—Since CaO-stabilized ZrO_2 is an oxygen ion conductor with an ionic transport number greater than 0.99 in the range of temperatures and oxygen partial pressures covered in this study, the open-circuit potentials of the solid-state cells are related to the standard Gibbs energy change for the corresponding cell reaction by the Nernst equation. The difference in the potentials of cells I and IV gives directly the Gibbs energy of formation of $PbO \cdot 6Al_2O_3$ from the component oxides. For the reaction

$$PbO(\text{orthorhombic}) + 6 \ \alpha\text{-}Al_2O_3 \rightarrow PbO \cdot 6Al_2O_3$$
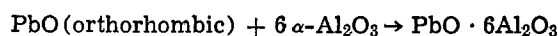
$$\Delta G° = -113,940 + 55.91T \ (\pm 200) \ \text{J mol}^{-1} \quad [6]$$

From the difference in the potentials of cells II and IV, the Gibbs energy change for the reaction,

$$5 \ PbO(\text{orthorhombic}) + PbO \cdot 6Al_2O_3(s)$$
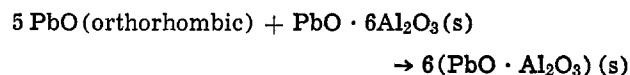
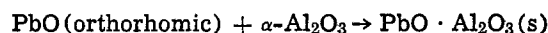$$\rightarrow 6(PbO \cdot Al_2O_3) \ (s)$$

is derived as

$$\Delta G° = -117,240 + 76.32T \ (\pm 200) \ \text{J mol}^{-1} \quad [7]$$

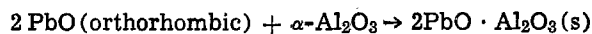Similarly, the difference in the potentials of cells III and IV gives, for the reaction

$$PbO(\text{orthorhombic}) + PbO \cdot Al_2O_3(s)$$
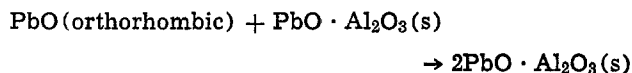
$$\rightarrow 2PbO \cdot Al_2O_3(s)$$

$$\Delta G° = -5480 + 2.15T \ (\pm 300) \ \text{J mol}^{-1} \quad [8]$$

From a rearrangement of the above equations, the free energies of formation of $PbO \cdot Al_2O_3$ and $2PbO \cdot Al_2O_3$ from component oxide can be readily calculated

$$PbO(\text{orthorhomic}) + \alpha\text{-}Al_2O_3 \rightarrow PbO \cdot Al_2O_3(s)$$

$$\Delta G° = -38,530 + 22.06T \ (\pm 50) \ \text{J mol}^{-1} \quad [9]$$

$$2 \ PbO(\text{orthorhombic}) + \alpha\text{-}Al_2O_3 \rightarrow 2PbO \cdot Al_2O_3(s)$$

$$\Delta G° = -44,010 + 24.21T \ (\pm 300) \ \text{J mol}^{-1} \quad [10]$$

The Gibbs energy, entropy, and enthalpy of mixing in the $PbO\text{-}Al_2O_3$ system are plotted in Fig. 5. The minimum value for the Gibbs energy of mixing at a mean temperature 1123 K occurs at the composition corresponding to the compound $PbO \cdot 6Al_2O_3$. The enthalpy of mixing, however, has a minimum value at the equimolar composition. The entropy of mixing is significantly negative for all three compounds, with a minimum at the equimolar composition.

The variation of the activity of PbO with composition in the $PbO\text{-}Al_2O_3$ system at 1123 K is shown in Fig. 6. The activity of PbO in the two phase region, $PbO \cdot 6Al_2O_3 + \alpha\text{-}Al_2O_3$, is 4.2×10^{-3}, which is very much lower than the corresponding activities of PbO in the $PbO\text{-}ZrO_2$ and $PbO\text{-}TiO_2$ system. The activity of PbO in the $PbZrO_3 + ZrO_2$ two-phase region is 0.24 and in the $PbTiO_3 + TiO_2$ phase field is 0.018 at 1123 K. Obviously, the compound $PbO \cdot 6Al_2O_3$ should form on the surface of alumina containers used in the processing of PZT ceramics at high temperatures. The activities of PbO corresponding to the formation of $PbO \cdot Al_2O_3$ and $2PbO \cdot Al_2O_3$ are higher than that prevailing in PZT ceramics. Therefore, these aluminates should not form, except as transient product
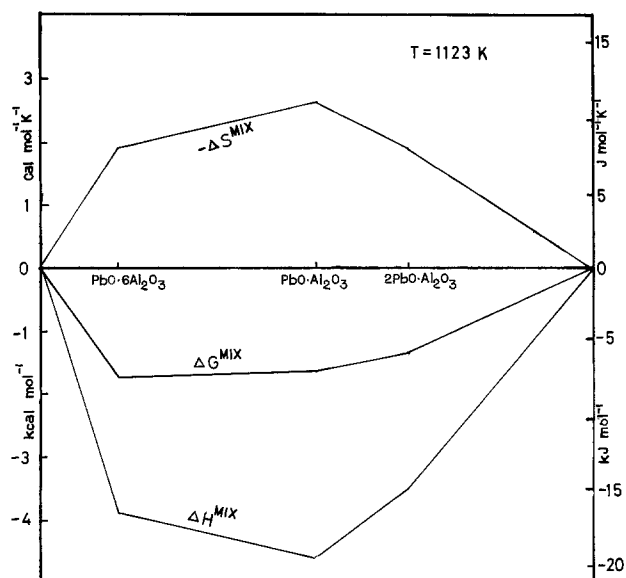
Fig. 5. The Gibbs energy, enthalpy, and entropy of mixing for PbO(yellow, s) — α Al$_2$O$_3$ system at 1123 K.

during the early stages of synthesis of PZT materials where unreacted PbO may be present.

Comparison with phase diagram.—The decomposition temperatures for lead aluminates shown on the phase diagrams for the PbO-Al$_2$O$_3$ system (3, 4) provide points of comparison with thermodynamic data obtained in this study. In the phase diagram of Torkar (3) based on DTA, the compound PbO · Al$_2$O$_3$ is shown to decompose at 1073 K into a mixture of PbO · 6Al$_2$O$_3$ and 2PbO · Al$_2$O$_3$. This reaction is not in conformity with the thermodynamic data obtained in this study, and appears to arise from an error in the interpretation of DTA traces, which show an exothermic peak corresponding to this temperature. The decomposition process must obviously give an endothermic peak.

In the phase diagram suggested by Kuxman and Fischer (4), (Fig 7), the compound 2PbO · Al$_2$O$_3$ is
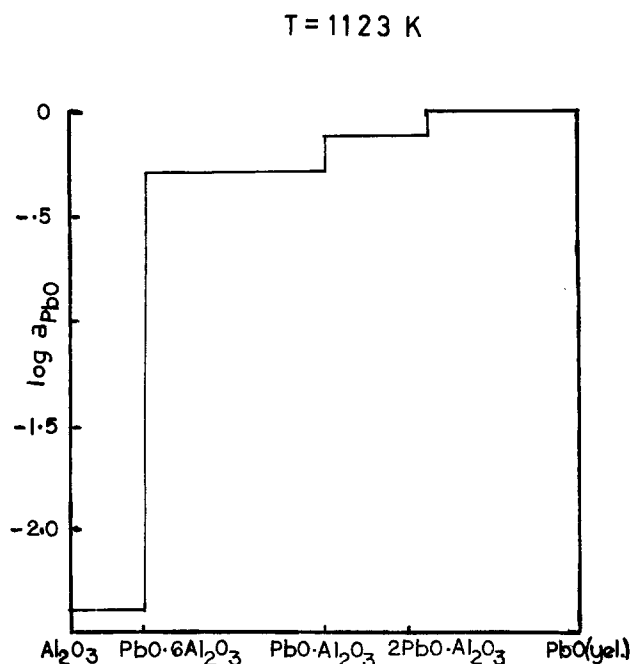
T = 1123 K

Fig. 6. The variation of the activity of PbO with composition in the PbO(yellow, s) — α Al$_2$O$_3$ system at 1123 K. The standard state for PbO is yellow form of solid PbO.
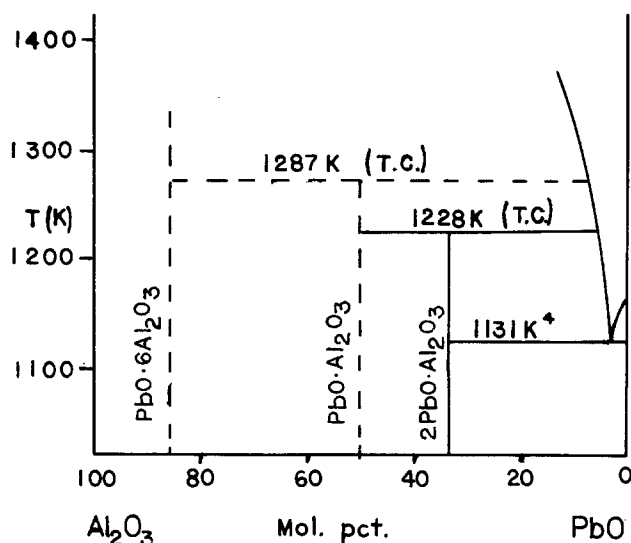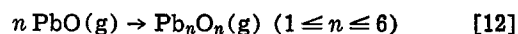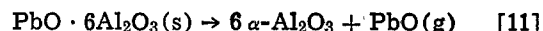

T.C. = Thermo. calculation

4 = Ref. 4

Fig. 7. Phase relations in the PbO-Al$_2$O$_3$ system suggested by Kuxman and Fischer (4).

shown to decompose at 1228 K into a mixture of PbO · Al$_2$O$_3$ and a liquid phase containing 94 m/o PbO. In good agreement with the phase diagram, the decomposition temperature calculated from the thermodynamic information is 1240 K. The calculation assumes that Raoult's law is valid for PbO activities in the liquid phase. The phase diagram (4) also suggests the decomposition of PbO · Al$_2$O$_3$ into a mixture of PbO · 6Al$_2$O$_3$ and liquid phase containing 92 m/o PbO at 1273 K. The calculated temperature for this reaction based on the thermodynamic information is 1287 K. If the activity of PbO in the liquid phase exhibits small negative deviations from Raoult's law, as might be expected in a system with strong compounds in the solid state, an even better agreement between the calculated· and phase diagram temperatures for the decomposition of PbO · Al$_2$O$_3$ and 2PbO · Al$_2$O$_3$ would result.

Partial pressures of vapor species over lead aluminates.—The vaporization of PbO · 6Al$_2$O$_3$ can be represented by the equations

$$PbO \cdot 6Al_2O_3(s) \rightarrow 6\,\alpha\text{-}Al_2O_3 + PbO(g) \qquad [11]$$

$$n\,PbO(g) \rightarrow Pb_nO_n(g) \quad (1 \leq n \leq 6) \qquad [12]$$

The equilibrium partial pressures of PbO and its polymeric forms are calculated from the Gibbs energies of formation for PbO · 6Al$_2$O$_3$, of vaporization for pure PbO and of polymerization reactions in the gas phase given by Drowart et al. (1) (Table I). The results are plotted in Fig. 8 as a function of the reciprocal of absolute temperature.

Similar vaporization reactions can be written for PbO · Al$_2$O$_3$ and 2PbO · Al$_2$O$_3$

Table I. Gibbs energies of vaporization of PbO and of polymerization reactions in the gas phase (1)

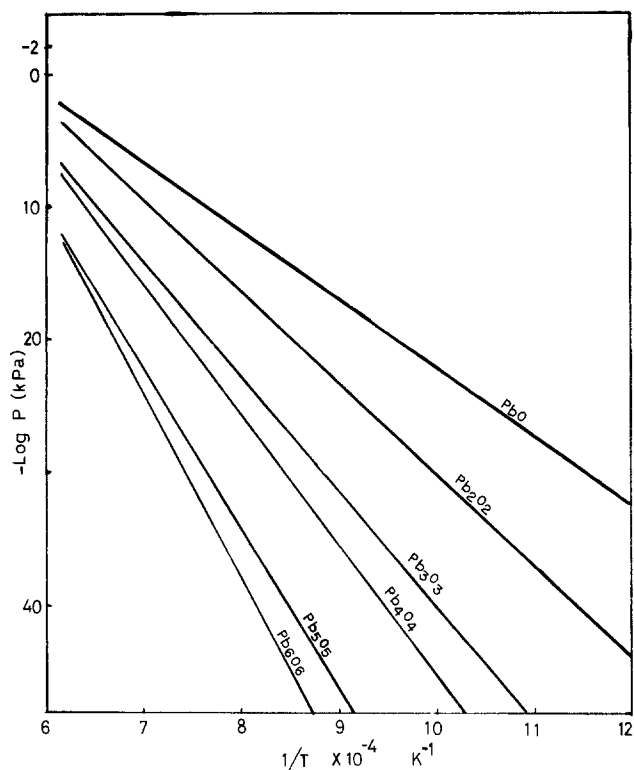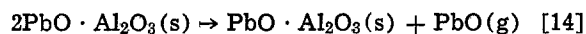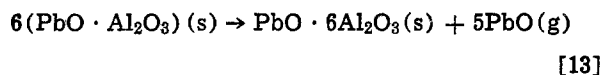| Reaction	$\Delta G°$, J
Pb$_n$O$_n$(g) $\rightarrow$ n PbO(g)	
$n = 2$	259,199 − 136.40T
$n = 3$	512,856 − 280.73T
$n = 4$	823,335 − 446.23T
$n = 5$	1,059,180 − 596.60T
$n = 6$	1,347,350 − 747.80T
PbO(s) $\rightarrow$ PbO(g)	278,805 − 153.97T

Fig. 8. The equilibrium partial pressures of different gas species containing PbO produced by vaporization of PbO · 6Al₂O₃.

$$6(PbO \cdot Al_2O_3)(s) \rightarrow PbO \cdot 6Al_2O_3(s) + 5PbO(g)$$

$$[13]$$

$$2PbO \cdot Al_2O_3(s) \rightarrow PbO \cdot Al_2O_3(s) + PbO(g) \quad [14]$$

The variation of the vapor compositions over these compounds with temperature is shown in Fig. 9 and 10. The relative importance of the polymeric species
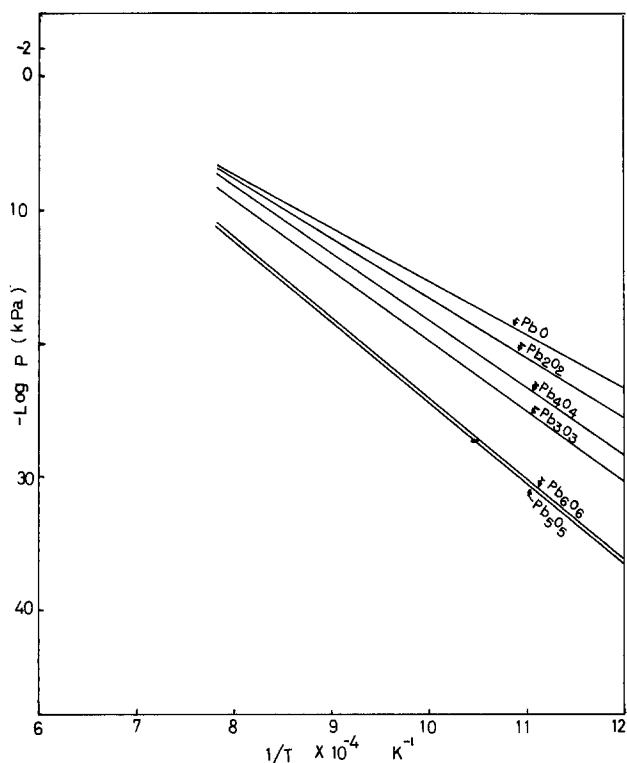

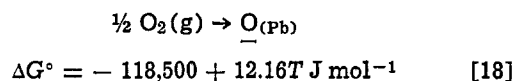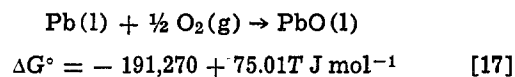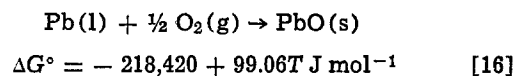**Fig. 9.** The partial pressures of monomeric and polymeric PbO species resulting from dissociation of PbO · Al₂O₃.
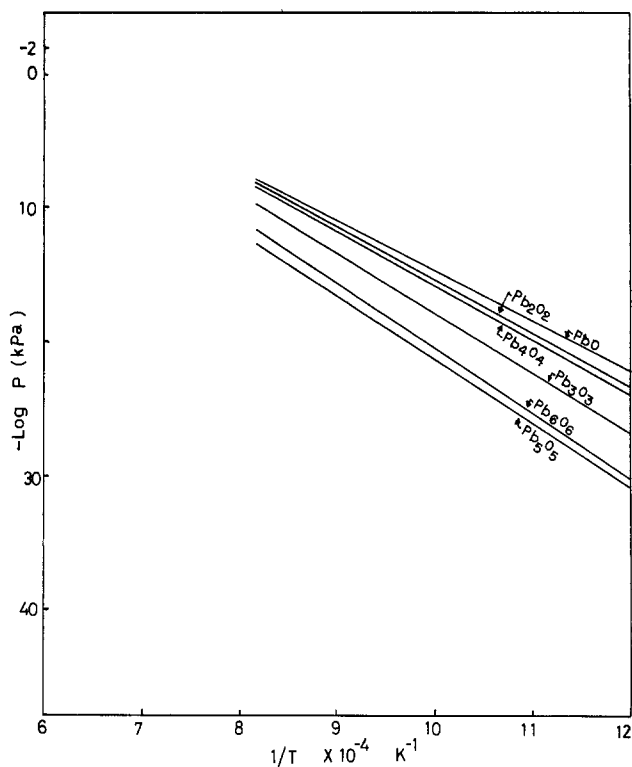
Fig. 10. The variation of partial pressure of PbO containing species obtained from equilibrium dissociation of 2PbO · Al₂O₃ with temperature.

in the gas phase increases with an increase in activity of PbO in the condensed phase.

Solubility of lead aluminates in liquid lead.—The dissolution of PbO · 6Al₂O₃ into liquid lead can be represented by the reaction

$$PbO \cdot 6Al_2O_3(s) \rightarrow 6\,\alpha\text{-}Al_2O_3 + \underline{O}_{(Pb)} + Pb(l) \quad [15]$$
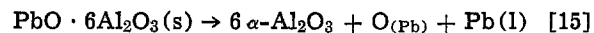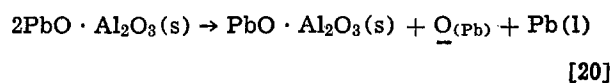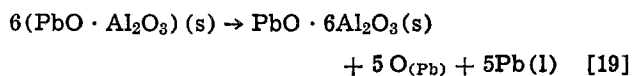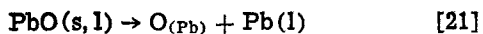
where $\underline{O}_{(Pb)}$ represents dissolved oxygen. It is convenient to choose the standard state for oxygen solute in liquid lead such that the activity of oxygen is equal to its concentration in atomic percent as the atomic percent approaches zero. The Gibbs energy change for reaction [15] can be evaluated from the results of this study for PbO · 6Al₂O₃, the free energy of formation of PbO and the free energy of solution of diatomic gaseous oxygen in liquid lead (7, 9)

$$Pb(l) + \tfrac{1}{2} O_2(g) \rightarrow PbO(s)$$

$$\Delta G^\circ = -218,420 + 99.06T \text{ J mol}^{-1} \qquad [16]$$

$$Pb(l) + \tfrac{1}{2} O_2(g) \rightarrow PbO(l)$$

$$\Delta G^\circ = -191,270 + 75.01T \text{ J mol}^{-1} \qquad [17]$$

$$\tfrac{1}{2} O_2(g) \rightarrow \underline{O}_{(Pb)}$$

$$\Delta G^\circ = -118,500 + 12.16T \text{ J mol}^{-1} \qquad [18]$$

The equilibrium constant for reaction [15] is equal to the atomic percent oxygen in liquid lead corresponding to the dissolution of PbO · 6Al₂O₃.

A similar analysis can be applied for the dissolution of PbO · Al₂O₃, 2PbO · Al₂O₃, and pure PbO in liquid lead. The relevant equations are

$$6(PbO \cdot Al_2O_3)(s) \rightarrow PbO \cdot 6Al_2O_3(s)$$

$$+ 5\,\underline{O}_{(Pb)} + 5Pb(l) \quad [19]$$

$$2PbO \cdot Al_2O_3(s) \rightarrow PbO \cdot Al_2O_3(s) + \underline{O}_{(Pb)} + Pb(l)$$

$$[20]$$

$$PbO(s, l) \rightarrow O_{(Pb)} + Pb(l) \qquad [21]$$

The equilibrium oxygen contents of liquid lead as result of the dissolution of pure PbO and the three aluminates are compared as a function of temperature in Fig. 11.

The partial pressure of PbO in a sintering atmosphere for PZT ceramics can be readily obtained from the measurement of the oxygen content of liquid lead exposed to the atmosphere using a solid-state cell. A knowledge of the oxygen content of lead established by a number of different chemical reactions can be profitably employed in identifying the pressure-controlling reaction under practical conditions.

Conclusion

The Gibbs energies of formation of lead aluminates from the component oxides have been determined using solid-state galvanic cells
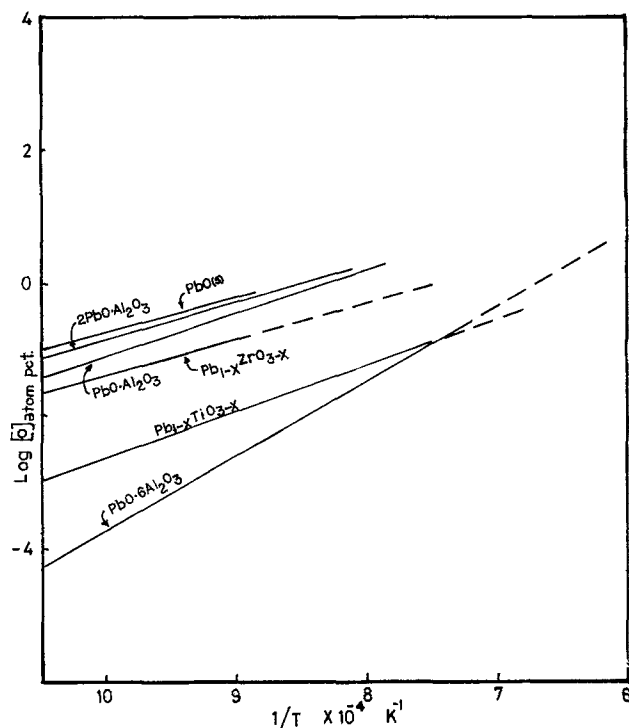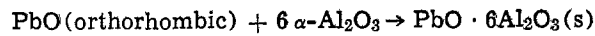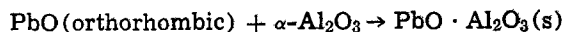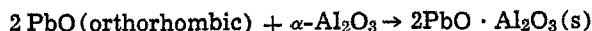

Fig. 11. The solubility of lead aluminates in liquid lead. The oxygen content of liquid lead in equilibrium with pure solid PbO, zirconia-saturated lead zirconate, and titania-saturated lead titanates are also shown for comparison.

$$PbO(orthorhombic) + 6\,\alpha\text{-}Al_2O_3 \rightarrow PbO \cdot 6Al_2O_3(s)$$

$$\Delta G^\circ = -113,940 + 55.91T \; (\pm 200) \text{ J mol}^{-1}$$

$$PbO(orthorhombic) + \alpha\text{-}Al_2O_3 \rightarrow PbO \cdot Al_2O_3(s)$$

$$\Delta G^\circ = -38,530 + 22.06T \; (\pm 50) \text{ J mol}^{-1}$$

$$2\,PbO(orthorhombic) + \alpha\text{-}Al_2O_3 \rightarrow 2PbO \cdot Al_2O_3(s)$$

$$\Delta G^\circ = -44,010 + 24.21T \; (\pm 300) \text{ J mol}^{-1}$$

These values are consistent with the phase diagram of Kuxman and Fischer (4) based on DTA and chemical analysis. The activity of PbO in $PbO \cdot 6Al_2O_3$ + $\alpha\text{-}Al_2O_3$ is 4.2×10^{-3} as compared to 0.24 for $Pb_{1-x}ZrO_{3-x} + ZrO_2$ and 0.018 for $Pb_{1-x}TiO_{3-x} + TiO_2$ at 1123 K. These values suggest the formation of $PbO \cdot 6Al_2O_3$ during the sintering of PZT ceramics in alumina crucibles at high temperatures.

The vapor phase in equilibrium with lead aluminates consists of a number of species which can be represented as Pb_nO_n $(1 \le n \le 6)$. The relative importance of the polymeric species in the gas phase increases with the activity of PbO in the condensed phase. The equilibrium oxygen content of liquid lead established by the dissolution of lead aluminates is evaluated from thermodynamic data.

REFERENCES

1. J. Drowart, R. Colin, and G. Exsteen, *Trans. Faraday Soc.*, **61**, 1376 (1965).
2. R. F. Geller and E. N. Bunting, *J. Res. Nat. Bur. Stand.*, **31**, Report 1564, 255 (1943).
3. V. K. Torkar, H. Krischner, and H. Moser, *Ber. Deutsche Keram. Ges.*, **43**, 259 (1966).
4. U. Kuxman and P. Fischer, *Erzmetall*, **27**, 533 (1974).
5. K. T. Jacob and W. W. Shim, *J. Am. Ceram. Soc.*, **64**, 573 (1981).
6. W. W. Shim and K. T. Jacob, *Can. Met. Q.*, In press.
7. K. T. Jacob and J. H. E. Jeffes, *Trans. Inst. Min. Metall.*, **80**, C32 (1971).
8. R. L. Ho'man and R. M. Fulrath, *J. Appl. Phys.*, **44**, 5227 (1973).
9. C. B. Alcock and T. N. Belford, *Trans. Faraday Soc.*, **60**, 822 (1964).